14 Nonlinear Information Fusion Algorithm of an Asynchronous Multisensor Based on the Cubature Kalman Filter

Wei Gao, Ya Zhang, and Qian Sun

CONTENTS

14.1 INTRODUCTION

Multisensor information fusion has been widely used in the military, defense, and high-tech fields. In multisensor information fusion theory, redundant and complementary information of multiple sensor measurements is used to improve system accuracy [1–4]. In practice, however, asynchronous information fusion problem are often encountered; for example, the sampling frequency and the inherent delay of sensors are different, and communication delays between sensors exist [5–8]. Improving system accuracy will be very difficult if the asynchronous problem cannot be solved effectively.

For asynchronous multisensor information fusion, a novel algorithm for multiple sensors with both space and time bias errors is proposed in Ref. [6], where a two-stage Kalman filtering (TSKF) and feedback system is applied to improve the entire estimation accuracy. But in this algorithm it is assumed that the sensors are independent, so the results are suboptimal. A new sequential asynchronous fusion algorithm is proposed in Ref. [8] by using the idea of sequential discretization of the sampling points on a continuous and distributed multisensor linear dynamic system. The algorithm avoids complicated calculation by using a first-come first serve criterion, but it requires information on all of the sensors to process, so it has a poor on-time performance. In consideration of the nonlinear model generated by the motion model, measurement model, and distributed measurement space transformation, the nonlinear filter must be selected when estimating the states of the multisensor information fusion system [4,9–12]. For the information fusion of a nonlinear asynchronous multisensor system, an optimal fusion framework of nonlinear multisensor data is proposed in Ref. [13]; the model is described more exactly to reduce errors. A nonlinear Stein-based estimation is proposed in Ref. [14] for wavelet de-noising of multichannel data, but the estimation results obtained with this method are suboptimal. A multisensor information fusion algorithm based on the extend Kalman filter (EKF) is proposed in Ref. [4], but the EKF solution approximates only to one order of the Taylor expansion, and the EKF needs to calculate the fuzzy Jacobian matrix, which increases the computational complexity. A multisensor asynchronous information fusion algorithm based on the unscented Kalman filter (UKF) is proposed in Ref. [11]. Compared with EKF, the filtering accuracy of UKF is higher, but the computational complexity is still a problem. In 2009, a more accurate nonlinear filtering solution based on the cubature transform named the cubature Kalman filter (CKF) was proposed by Arasaratnam and Haykin [15–19]. The CKF solution uses cubature points to approximate the mean and variance of the nonlinear system so third-order accuracy of the system can be achieved. This method has a higher accuracy and requires less calculation.

In this chapter, a nonlinear fusion algorithm for asynchronous multisensor data is presented. The nonlinear characteristics are considered while the asynchronous multisensor fusion problem is solved according to Ref. [2]. Simulation results confirm the effectiveness of the proposed algorithm.

14.2 BACKGROUND

14.2.1 Information Fusion of a Multisensor

Because the distributed processing can extend the flexibility of multisensor measuring system parameter estimation and also enhance the viability of the system [1,20], it is used in this chapter. Consider the following state equation of a discrete-time dynamic system:

$$\hat{x}(k) = \Phi(k, k-1)\hat{x}(k-1) + w(k-1) \tag{14.1}$$

where k indicates the the discrete time; $\hat{x}(k)$ is the systemic state vector at time k; $\Phi(k, k-1)$ is the systemic state transfer matrix; $w(k-1)$ is a zero-mean Gaussian white noise process; and $w \sim (0, Q)$.

The measurement equation constituted by N asynchronous sensors is

$$z_i(k) = H_i\hat{x}(k) + v_i(k) \tag{14.2}$$

where $i = 1, 2, \ldots, N$ is the ith measurement at time k; H_i is the ith measurement matrix; $v_i(k)$ is the ith zero-mean Gaussian white noise; and $v \sim (0, R_i)$.

If information from i sensors is measured simultaneously, each sensor obtains the optimal estimation locally utilizing its filter first, and then the fusion center weights all estimated results of the sensors. The framework of multisensor information fusion is shown in Figure 14.1.

Assume that the estimated value of the state at time k can be represented by a linear combination of each sensor's state estimation. Then we have

$$\hat{x}(k) = D_1\hat{x}_1(k_1) + D_2\hat{x}_2(k_2) + \ldots + D_i\hat{x}_i(k_i) \tag{14.3}$$

where $D_1, D_2, \ldots, D_i$ are the corresponding weights of sensors.

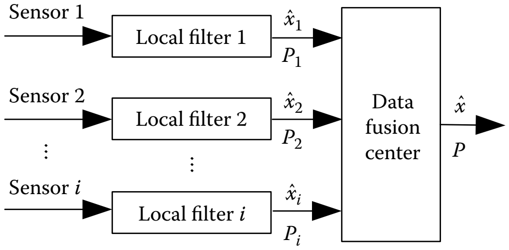

FIGURE 14.1 The framework of multisensor information fusion.

Taking the expectation of Equation 14.3, we have

$$E[\hat{x}(k)] = D_1\Phi^{-1}(k,k_1)E[x(k)] + \ldots + D_i\Phi^{-1}(k,k_i)E[x(k)]$$

If we define

$$S_1 = D_1\Phi^{-1}(k, k_1),\ldots, S_i = D_i\Phi^{-1}(k, k_i) \tag{14.4}$$

then

$$P(k) = E\{[S_1\tilde{x}_1(k|k_1) + \ldots + S_i\tilde{x}_i(k|k_i)][S_1\tilde{x}_1(k|k_1) + \ldots + S_i\tilde{x}_i(k|k_i)]^T\}$$

According to Ref. [6], $\hat{x}(k)$ is an unbiased estimation, when

$$D_1\Phi^{-1}(k, k_1) + D_2\Phi^{-1}(k, k_2) + \ldots + D_2\Phi^{-1}(k, k_2) = I$$

We define

$$\begin{aligned} A_1 &= P_1(k|k_1) + P_1^T(k|k_1) \\ &\vdots \\ A_i &= P_i(k|k_i) + P_i^T(k|k_i) \end{aligned}$$

When the sensors are independent, the filtering results are locally optimal when

$$\begin{aligned} S_1 &= \left(I + \sum_{i=2}^{N-1}\left(A_1A_i^{-}1\right) + A_1A_N^{-}1 \right)^{-1} \\ S_2 &= S_1A_1A_2^{-1} \\ &\vdots \\ S_i &= S_iA_1A_i^{-1} \end{aligned} \tag{14.5}$$

We can obtain each D_1, D_2, …, D_i by Equations 14.4 and 14.5, and then the optimal state estimation of multisensor information fusion can also be obtained.

14.2.2 CKF Filter Solution

Consider the following discrete-time nonlinear state-space model

$$\begin{cases} x(k) = f(x(k-1)) + w(k-1) \\ z(k) = h(x(k)) + v(k) \end{cases} \tag{14.6}$$

where $x(k)$ is the state of the system at time k; $z(k)$ is the measurement at time k; $f(\cdot)$ and $h(\cdot)$ are some known nonlinear functions; and $w(k-1)$ and $v(k)$ are noise samples from two independent zero-mean Gaussian processes with covariance $Q(k-1)$ and $R(k)$, respectively.

CKF is proposed to solve the nonlinear filtering problem based on the spherical-radial cubature criterion. CKF first approximates the mean and variance of probability distribution through cubature points with the same weight, propagates the cubature points shown earlier by the nonlinear function, and calculates the mean and variance of the current approximation Gaussian distribution by the propagated cubature points.

The set of $2n$ cubature points are given by $[\xi_i, \omega_i]$, where ξ_i is the ith cubature point and ω_i is the corresponding weight.

$$\begin{cases} \xi_i = \sqrt{n}[1]_i \\ \omega_i = \dfrac{1}{2n} \end{cases} \tag{14.7}$$

where $i = 1, 2, \ldots, 2n$ and n is the dimension of the nonlinear system.

The steps involved in the time update and the measurement update of CKF are summarized as follows [18]. Assuming that at time $k - 1$ the posterior density is known.

$$p(x(k-1)) = N(\hat{x}(k-1|k-1), P(k-1|k-1)) \tag{14.8}$$

1. CKF: Time update

$$P(k-1|k-1) = S(k-1|k-1)S(k-1|k-1)^T \tag{14.9}$$

$$\xi_i(k-1|k-1) = S(k-1|k-1)\xi_i + \hat{x}(k-1|k-1) \tag{14.10}$$

$$\gamma_i(k|k-1) = f(\xi_i(k-1|k-1)) \tag{14.11}$$

$$\hat{x}(k|k-1) = \frac{1}{2n}\sum_{i=1}^{2n}\gamma_i(k|k-1) \tag{14.12}$$

$$P(k|k-1) = \frac{1}{2n}\sum_{i=1}^{2n}\gamma_i(k|k-1)\gamma_i(k|k-1)^T - \hat{x}(k|k-1)\hat{x}(k|k-1)^T + Q(k-1) \tag{14.13}$$

2. CKF: Measurement update

$$P(k|k-1) = S(k|k-1)S(k|k-1)^T \tag{14.14}$$

$$\xi_i(k|k-1) = S(k|k-1)\xi_i + \hat{x}(k|k-1) \tag{14.15}$$

$$\chi_i(k|k-1) = h(\xi_i(k|k-1)) \tag{14.16}$$

$$\hat{z}(k|k-1) = \frac{1}{2n}\sum_{i=1}^{2n}\chi_i(k|k-1) \tag{14.17}$$

$$P_{zz}(k|k-1) = \frac{1}{2n}\sum_{i=1}^{2n}\chi_i(k|k-1)\chi_i(k|k-1)^T - \hat{z}(k|k-1)\hat{z}(k|k-1)^T + R(k) \quad (14.18)$$

$$P_{xz}(k|k-1) = \frac{1}{2n}\sum_{i=1}^{2n}\xi_i(k|k-1)\chi_i(k|k-1)^T - \hat{x}(k|k-1)\hat{z}(k|k-1)^T \quad (14.19)$$

So the filter gain is

$$K(k) = P_{xz}(k|k-1)(P_{zz}(k|k-1))^{-1} \quad (14.20)$$

The filter state and the state error covariance are

$$\hat{x}(k|k) = \hat{x}(k|k-1) + K(k)(z(k) - \hat{z}(k|k-1)) \quad (14.21)$$

$$P(k|k) = P(k|k-1) - K(k)P_{zz}(k|k-1)K(k)^T \quad (14.22)$$

The CKF used a third-degree cubature rule to numerically compute the mean and variance of the probability distribution with cubature points, so the estimation accuracy can achieve third order or higher. Furthermore, this filtering solution no longer needs to calculate Jacobians and Hessians, and thus the computational complexity and consumption will decrease significantly. In a nutshell, the CKF is a new and improved algorithmic addition to the toolkit for nonlinear filtering.

14.3 NONLINEAR INFORMATION FUSION ALGORITHM OF AN ASYNCHRONOUS MULTISENSOR BASED ON CKF

In the information fusion problem of an asynchronous multisensor, considering the discrete-time nonlinear state-space model shown by Equation 14.6, we use CKF in data fusion. For asynchronous multisensor information fusion, we combine the multisensor data into something like single-sensor data with the time subdivision method. The sampling interval of the ith sensor is T, the corresponding discrete time is marked k_i, and the sampling interval of the information fusion center is denoted as T. The principle of multisensor asynchronous sampling is shown in Figure 14.2.

At some time intervals, data of only one sensor are measured, and the measurement data of the sensor will be directly used in the filtering process. At some time intervals, data of more than one sensor are measured, so we estimate every sensor state respectively, and then weight the filtering results. At some time intervals, there are no sensor data, and we only time update the estimation results of the previous time as the estimation results at this time. A flowchart of the proposed nonlinear information fusion algorithm based on CKF is shown in Figure 14.3.

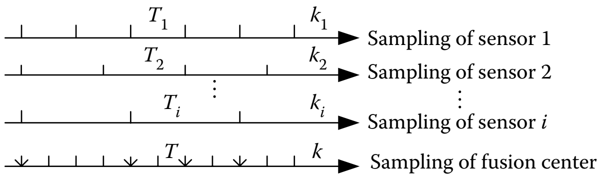

FIGURE 14.2 The principle of multisensor asynchronous sampling.

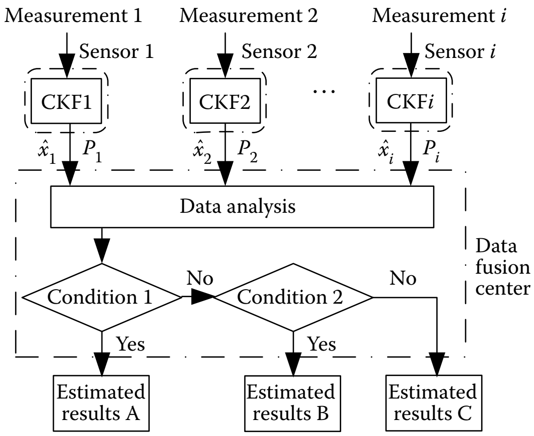

FIGURE 14.3 Flowchart of a nonlinear asynchronous multisensor information fusion algorithm based on CKF.

In Figure 14.3, *Condition 1* means that at the current time the data of only one sensor can be measured; *Condition 2* means that at the current time the data of multiple sensors can be measured; *Estimated results A* refers to the estimated results of the sensor; *Estimated results B* refers to the weight of the estimated results of all sensors; *Estimated results C* is the time update of the estimated results from the previous moment.

The algorithm is summarized as follows.

1. At some time intervals, data of only one sensor are measured, and the measurement data of the sensor will be directly filtered based on the CKF. The fusion state estimation is the optimal estimated state values.

$$\hat{x}(k) = \hat{x}_i(k_i) \tag{14.23}$$

2. At some time intervals, data of more than one sensor are measured, so we estimate every sensor state respectively, and then weight the filtering results. The fusion state estimation is shown by

$$\hat{x}(k) = D_1\hat{x}_1(k_1) + D_2\hat{x}_2(k_2) + \ldots + D_i\hat{x}_i(k_i) \tag{14.24}$$

where $D_1, D_2, \ldots, D_i$ can be calculated according to Section 14.2.1.

3. At some time intervals, there are no sensor data and we only time update the estimation results from previous time. The fusion state estimation is

$$\hat{x}(k) = \hat{x}(k|k-1) \tag{14.25}$$

This new algorithm increases the observation data of the target by using sensor observation, and thereby the estimation accuracy of the multisensor system of the measurement parameters can be improved. In addition, the total computational complexity is moderated utilizing CKF. Thus, this algorithm can handle the nonlinear information fusion problems of an asynchronous multisensor system, and the effectiveness and viability of the system can be enhanced with this algorithm.

14.4 SIMULATION RESULTS

To illustrate the performance of the proposed fusion algorithm, numerical simulation examples are given in this section. Consider the discrete-time dynamic state equation of the target track:

$$x(k) = \begin{bmatrix} 1 & \dfrac{\sin \Omega\Delta}{\Omega} & 0 & \dfrac{\cos \Omega\Delta - 1}{\Omega} \\ 0 & \cos \Omega\Delta & 0 & -\sin \Omega\Delta \\ 0 & \dfrac{1-\cos \Omega\Delta}{\Omega} & 1 & \dfrac{\sin \Omega\Delta}{\Omega} \\ 0 & \sin \Omega\Delta & 0 & \cos \Omega\Delta \end{bmatrix} x(k-1) + w(k-1) \tag{14.26}$$

where the systemic state vector is $x = [x\ \dot{x}\ y\ \dot{y}]^T$, x and y denote the positions of the target, and $\dot{x}$, $\dot{y}$ denote the velocities of the target; Δ is the time step between measurements; Ω is the angular rate of the target and $\Omega = 3°/\text{s}$; and the process noise $w(k) \sim N(0, Q)$ with a covariance $Q = \text{diag}[qM \quad qM]$, where $q = 0.1$ and $M = \Delta^3/3\Delta^2/2\Delta^2/2\Delta$.

We consider two asynchronous sensors to observe the target. These two sensors are fixed and equipped to measure the range and bearing. Hence, we write the measurement equation

$$\begin{bmatrix} r_i(k) \\ \theta_i(k) \end{bmatrix} = \begin{bmatrix} \sqrt{x_i(k)^2 + y_i(k)^2} \\ \arctan(y_i(k)/x_i(k)) \end{bmatrix} + v_i(k)$$

where $i = 1, 2$ and the corresponding measurement noise is $v_i(k) \sim N(0, R_i)$ with $R_1 = \text{diag}[r_1\sigma_\gamma \quad r_1\sigma_\theta]$ and $R_2 = \text{diag}[r_2\sigma_\gamma \quad r_2\sigma_\theta]$, where $\sigma_\gamma = 10$ m, $\sigma_\theta = \sqrt{10}$ mrad, $r_1 = 0.5$, $r_2 = 1$.

The initial state and the associated covariance are

$$x_0 = [100\text{ m} \quad 10\text{ m/s} \quad 100\text{ m} \quad 10\text{ m/s}]$$

$$P_0 = \text{diag}[100\text{ m}^2 \quad 10\text{ m}^2/\text{s}^2 \quad 100\text{ m}^2 \quad 10\text{m}^2/\text{s}^2]$$

The initial state estimate $\hat{x}_0$ is chosen randomly from $N(x_0, P_0)$ in each run; the sampling interval of sensor 1 is $T_1 = 2$ s and the sampling interval of sensor 2 is $T_2 = 3$ s, so the sampling interval of the fusion center is $T_0 = T_1 - T_2 = 1$ s. The total time of each run is 100 s.

To track the maneuvering aircraft, comparing its performance against the CKF using only the data of sensor 1 and the CKF using only the data of sensor 2, we use the novel algorithm of nonlinear asynchronous data fusion based on the CKF. For a fair comparison, we make 50 independent Monte Carlo runs. All nonlinear filters are initialized with the same condition in each run.

To compare various performances, we use the root mean square error (RMSE) of the position and velocity. The RMSE yields a combined measure of the bias and variance of filter estimation. We define the RMSE in position and velocity at time k as

$$\mathrm{PMSE}_{\mathrm{pos}}(k) = \sqrt{\frac{1}{N}\sum_{n=1}^{N}((x_n(k) - x_n(k|k))^2 + (y_n(k) - y_n(k|k))^2)}$$

$$\mathrm{PMSE}_{\mathrm{vel}}(k) = \sqrt{\frac{1}{N}\sum_{n=1}^{N}((\dot{x}_n(k) - \dot{x}_n(k|k))^2 + (\dot{y}_n(k) - \dot{y}_n(k|k))^2)}$$

where $x_n(k)$, $y_n(k)$ and $x_n(k|k)$, $y_n(k|k)$ are the true and estimated positions at the nth Monte Carlo run. Similarly, $\dot{x}_n(k)$, $\dot{y}_n(k)$ and $\dot{x}_n(k|k)$, $\dot{y}_n(k|k)$ are the true and estimated velocities at the nth Monte Carlo run. N is the total number of Monte Carlo runs.

Figures 14.4 and 14.5 show the estimated RMSE of position and velocity, respectively for CKF using only the data of sensor 1, CKF using only the data of sensor 2, and the proposed fusion algorithm with two sensors. As can be seen from Figures 14.4 and 14.5, the proposed new fusion algorithm is superior to the CKF using only a single sensor in the target track model.

We use the novel algorithm based on the CKF (algorithm 1) for its numerical stability and compare it with the nonlinear fusion algorithm of the asynchronous sensors based on UKF (algorithm 2) introduced in Ref. [11]. We also make 50 independent Monte Carlo runs and the nonlinear filters are initialized with the same condition in each run. Figures 14.6 and 14.7 show the estimated RMSE in position and velocity, respectively for the proposed nonlinear fusion algorithm based on CKF (algorithm 1) and the algorithm based on UKF (algorithm 2).

The simulation results show that the accuracy of the proposed new algorithm based on the CKF is higher than that of the existing algorithm based on UKF. The main reason is that UKF gets the sigma points and corresponding weights by unscented transformation (UT), and the weights are often negative in a high-dimension system, which will introduce high-order truncation error items, reducing the accuracy of the algorithm. CKF obtains the cubature points and propagates them via the nonlinear equations; thus the weights are always positive and the errors are decreased significantly. So the numerical stability and the filtering accuracy of the novel algorithm are all better than those of the existing algorithm.

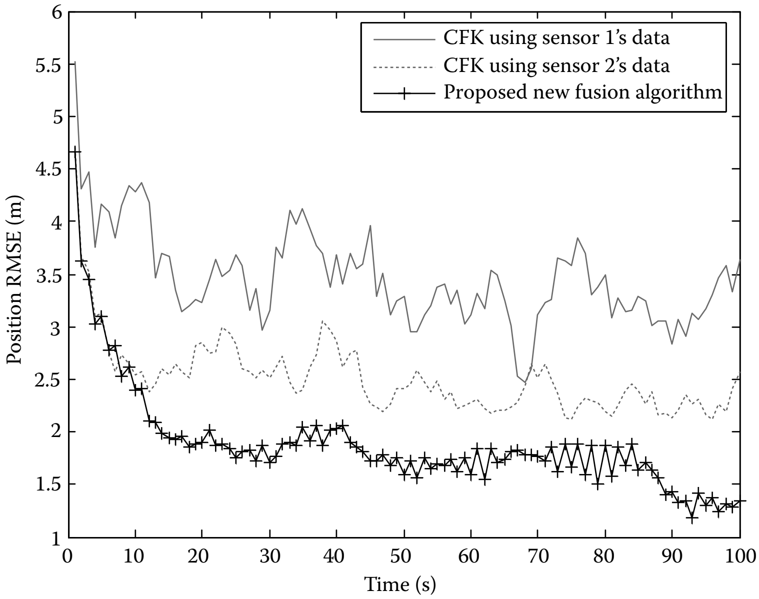

FIGURE 14.4 Position RMSEs across 50 Monte Carlo runs.

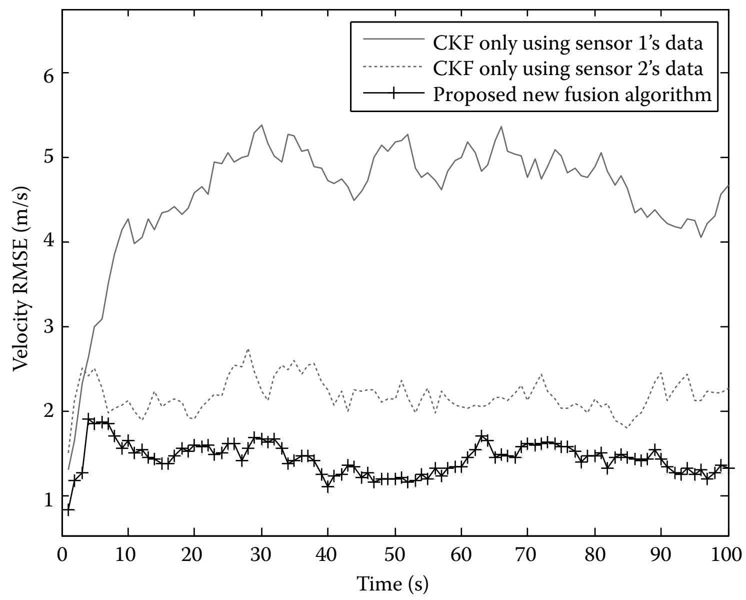

FIGURE 14.5 Velocity RMSEs across 50 Monte Carlo runs.

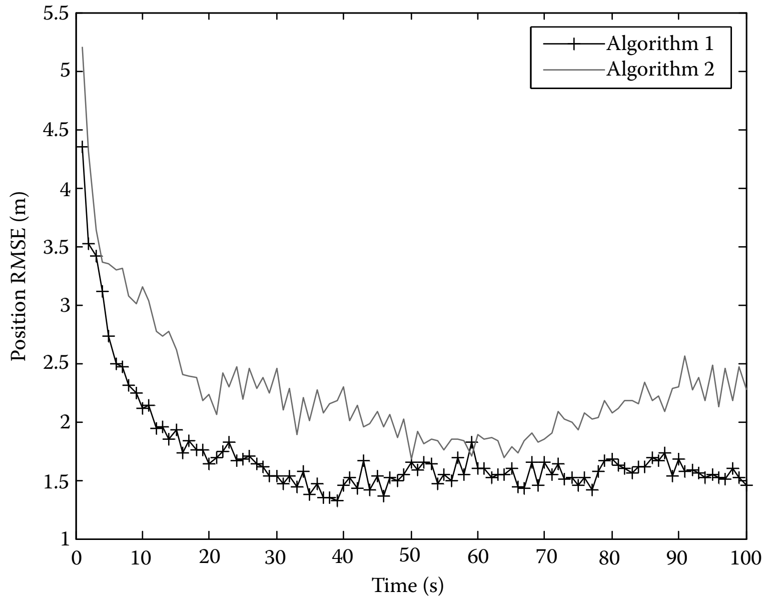

FIGURE 14.6 Position RMSEs of algorithms 1 and 2.

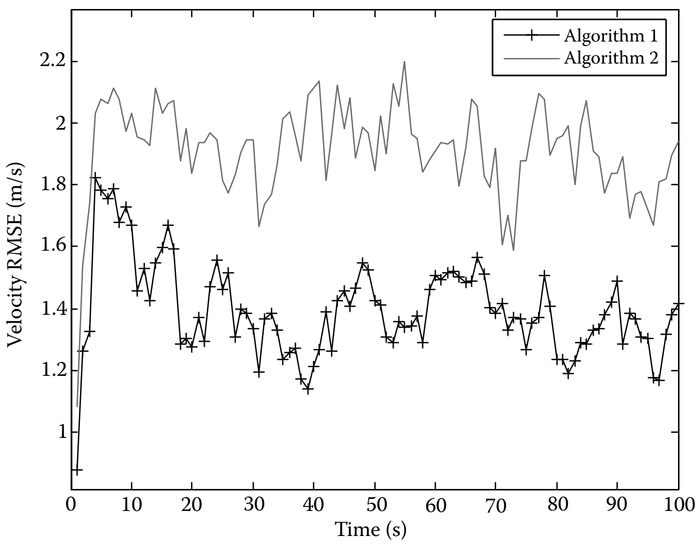

FIGURE 14.7 Velocity RMSEs of algorithms 1 and 2.

14.5 CONCLUSIONS

A new and efficient fusion algorithm of nonlinear asynchronous multisensor information based on CKF has been developed and its performances were demonstrated by numerical simulations. Compared with CKF using information from every single sensor, simulation results show that the derived fusion algorithm could fuse the information of a nonlinear asynchronous multisensor efficiently. The estimated accuracy of the systemic states is improved by utilizing the new algorithm. However, we supposed that each of the sensors is independent, and we have not discussed the algorithm in the case of correlated noise, which will be the focus of future research.

REFERENCES

1. Z.-T. Hu, X.-X. Liu, and Y. Jin. Multi-sensor observation of adaptive Rao-Blackwellised particle filtering algorithm. *Systems Engineering and Electronics*, 2:16, 2012.
2. Y. Hu, Z. Duan, and D. Zhou. Estimation fusion with general asynchronous multi-rate sensors. *Aerospace and Electronic Systems, IEEE Transactions on*, 46(4):2090–2102, 2010.
3. J. C. Zavala-Diaz, O. Diaz-Parra, J. A. Hernandez-Aguilar, and J. Perez Ortega. Mathematical linear multi-objective model with a process of neighbourhood search and its application for the selection of an investment portfolio in the Mexican stock exchange during a period of debacle. *Advances in Information Sciences and Service Sciences*, 3(4):89–99, 2011.
4. X. Xu, H. Zhang, and X. Tang. Micro-EKF fusion algorithm for multi-sensor systems with correlated noise. *Qinghua Daxue Xuebao/Journal of Tsinghua University*, 52(9):1199–1204, 2012.
5. X. Yu, and J. Yi-Hui. Asynchronous suboptimal fusion of correlated target tracks from multisensors. *Systems Engineering and Electronics*, 25(11):1318–1320, 1440, 2003.
6. Y. Ma, and P. Niu. Based on multi-sensor information fusion circulating fluidized bed boiler combustion process clustering control research. *Advances in Information Sciences & Service Sciences*, 4(3):35–43, 2012.
7. M. Lv, W. Hou, and X. Tian. The method of virtual driving behavior in active safety based on information fusion. *Advances in Information Sciences and Service Sciences*, 4(11):337–343, 2012.
8. S. Feng, and S. Wei. Research on calibration of IFOG based on two-axis indexing. *Control and Decision*, 26(3):346–350, 2011.

9. U. Rashid, H. D. Tuan, P. Apkarian, and H. H. Kha. Globally optimized power allocation in multiple sensor fusion for linear and nonlinear networks. *IEEE Transactions on Signal Processing*, 60(2):903–915, 2012.
10. S. Gundimada, and V. K. Asari. Facial recognition using multisensor images based on localized kernel eigen spaces. *IEEE Transactions on Image Processing*, 18(6):1314–1325, 2009.
11. M. Li, Y.-F. He, and F.-Z. Nian. An improved particle filter algorithm and its performance analysis. *Advances in Information Sciences and Service Sciences*, 4(23):547–555, 2012.
12. W. Gao, Y. Zhang, and J. Wang. A strapdown interial navigation system/beidou/doppler velocity log integrated navigation algorithm based on a cubature Kalman filter. *Sensors*, 14(1):1511–1527, 2014.
13. S. Suranthiran, and S. Jayasuriya. Optimal fusion of multiple nonlinear sensor data. *IEEE Sensors Journal*, 4(5):651–663, 2004.
14. C. Chaux, L. Duval, A. Benazza-Benyahia, and J.-C. Pesquet. A nonlinear stein-based estimator for multichannel image denoising. *IEEE Transactions on Signal Processing*, 56(8 II):3855–3870, 2008.
15. I. Arasaratnam, and S. Haykin. Cubature Kalman filters. *IEEE Transactions on Automatic Control*, 54(6):1254–1269, 2009.
16. I. Arasaratnam, S. Haykin, and T. R. Hurd. Cubature Kalman filtering for continuous-discrete systems: Theory and simulations. *IEEE Transactions on Signal Processing*, 58(10):4977–4993, 2010.
17. K. Pakki, B. Chandra, D.-W. Gu, and I. Postlethwaite. Cubature information filter and its applications. pp. 3609–3614, In *Proceedings of the 2011 American Control Conference, (ACC 2011)*. June 29th–July 1st, 2011, San Francisco, 2011.
18. I. Arasaratnam, and S. Haykin. Cubature Kalman smoothers. *Automatica*, 47(10):2245–2250, 2011.
19. F. Yu, and Q. Sun. Angular rate optimal design for the rotary strap-down inertial navigation system. *Sensors*, 14(4):7156–7180, 2014.
20. Z. Hua, Z. Youguang, and L. Guoyan. Particle-filtering-based approach to undetermined blind separation. *Advances in Information Sciences and Service Sciences*, 4(6):305–313, 2012.